

Supporting information

Tetragonal Tungsten Bronze Type Sn(II)-Based Quaternary Oxides: A New Type of Visible-Light- Absorbing Semiconductors for Photoelectrochemical Water Oxidation

Yalong Zou^{a,#}, Jiabo Le^{a,#}, Yufeng Cao^a, Na An^a, Yang Zhou^a, Jianming Li^c,

Deyu Liu^{a,b,*} and Yongbo Kuang^{a,b*}

- a. Ningbo Institute of Materials Technology and Engineering, Chinese Academy of Sciences, Ningbo 315201, Zhejiang, China*
- b. Center of Materials Science and Optoelectronics Engineering, University of Chinese Academy of Sciences, Beijing 100049, China*
- c. Research Center of New Energy, Research Institute of Petroleum Exploration & Development (RIPED), PetroChina, Beijing, 100083, China*

These authors contributed equally to this work.

Author Information

Corresponding Authors:

Deyu Liu – Ningbo Institute of Materials Technology and Engineering, Chinese Academy of Sciences, Ningbo 315201, China; Center of Materials Science and Optoelectronics Engineering, University of Chinese Academy of Sciences, Beijing 100049, China; Email: liudeyu@nimte.ac.cn

Yongbo Kuang – Ningbo Institute of Materials Technology and Engineering, Chinese Academy of Sciences, Ningbo 315201, China; Center of Materials Science and Optoelectronics Engineering, University of Chinese Academy of Sciences, Beijing 100049, China; orcid.org/0000-0002-0079-3720; Phone: +86-574-86686931; Email: kuangyongbo@nimte.ac.cn

Results and Discussion

Table S1 Mesophase identification and corresponding synthesis conditions

Sample	Amount of K ₂ CO ₃ (mmol)	Synthesis temperature (°C)
K-Pyro-900-1.2 *	1.2	900
K-TTB-1100-1.2	1.2	1100
K-TTB-1300-1.2	1.2	1300
K-TTB-1300-1.5	1.5	1300
K-TTB-1300-2.0 *	2.0	1300
K-TTB-1300-2.2	2.2	1300

Footnote: The two samples marked with * represent the two samples (Pyro and TTB) appearing in the maintext and the following tables and figures.

Table S2 XRF profile of K-TTB

Element	Wt %	Atomic percent
K	17.9	50.3
Ta	59.5	36.2
W	22.6	13.5
Total content:	100.0	100.0

Table S3 XRF profile of K-Pyro

Element	Wt %	Atomic percent
K	10.3	34.5
Ta	41.6	30.6
W	48.3	34.9
Total content:	100.0	100.0

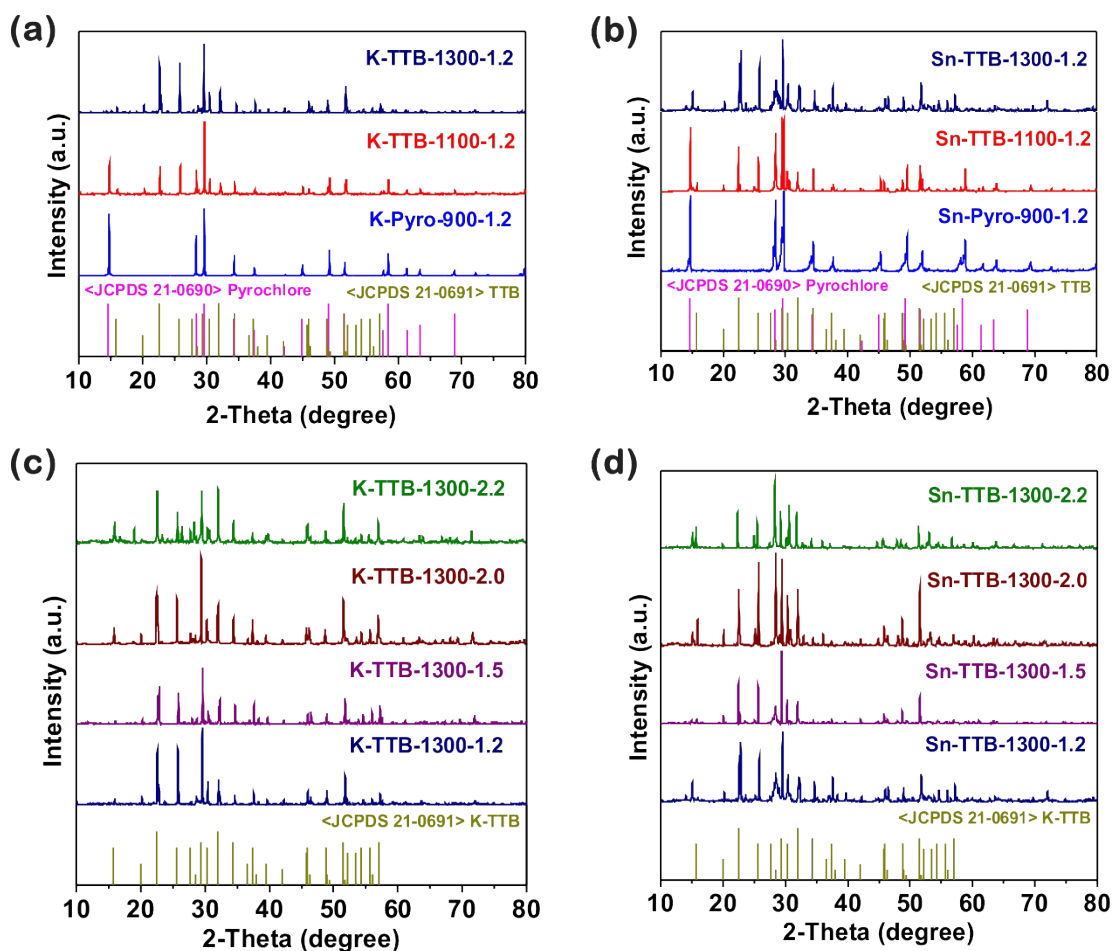


Figure S1. XRD patterns of K-precursors and Sn-products, (a, c) K-Pyro and K-TTB, (b, d) Sn-Pyro and Sn-TTB. The K-precursors were synthesized by the solid-state reaction under different temperatures and raw ratios.

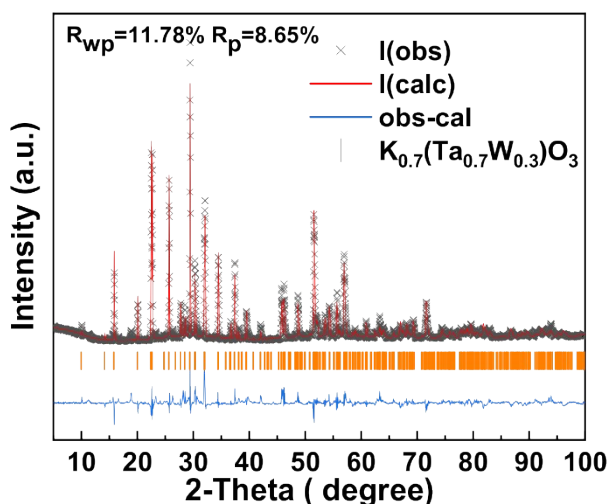


Figure S2. Rietveld refinement of K-TTB ($K_{0.7}(Ta_{0.7}W_{0.3})O_3$, Tetragonal, P 4/m b m): experimental data (black), simulated diffraction (red), position of observed diffractions (orange), and residual plot (blue).

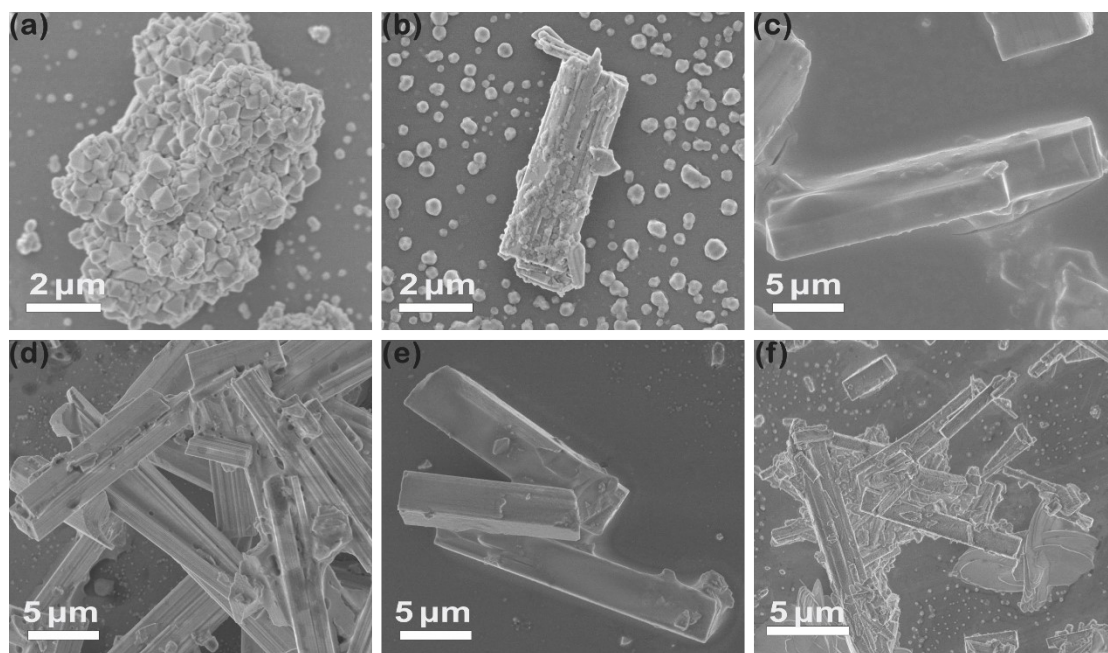


Figure S3. SEM images of K- precursors prepared at different temperatures and with varied K/Ta ratios, (a) K-Pyro-900-1.2, (b) K-TTB-1100-1.2, (c) K-TTB-1300-1.2, (d) K-TTB-1300-1.5, (e) K-TTB-1300-2.0, (f) K-TTB-1300-2.2.

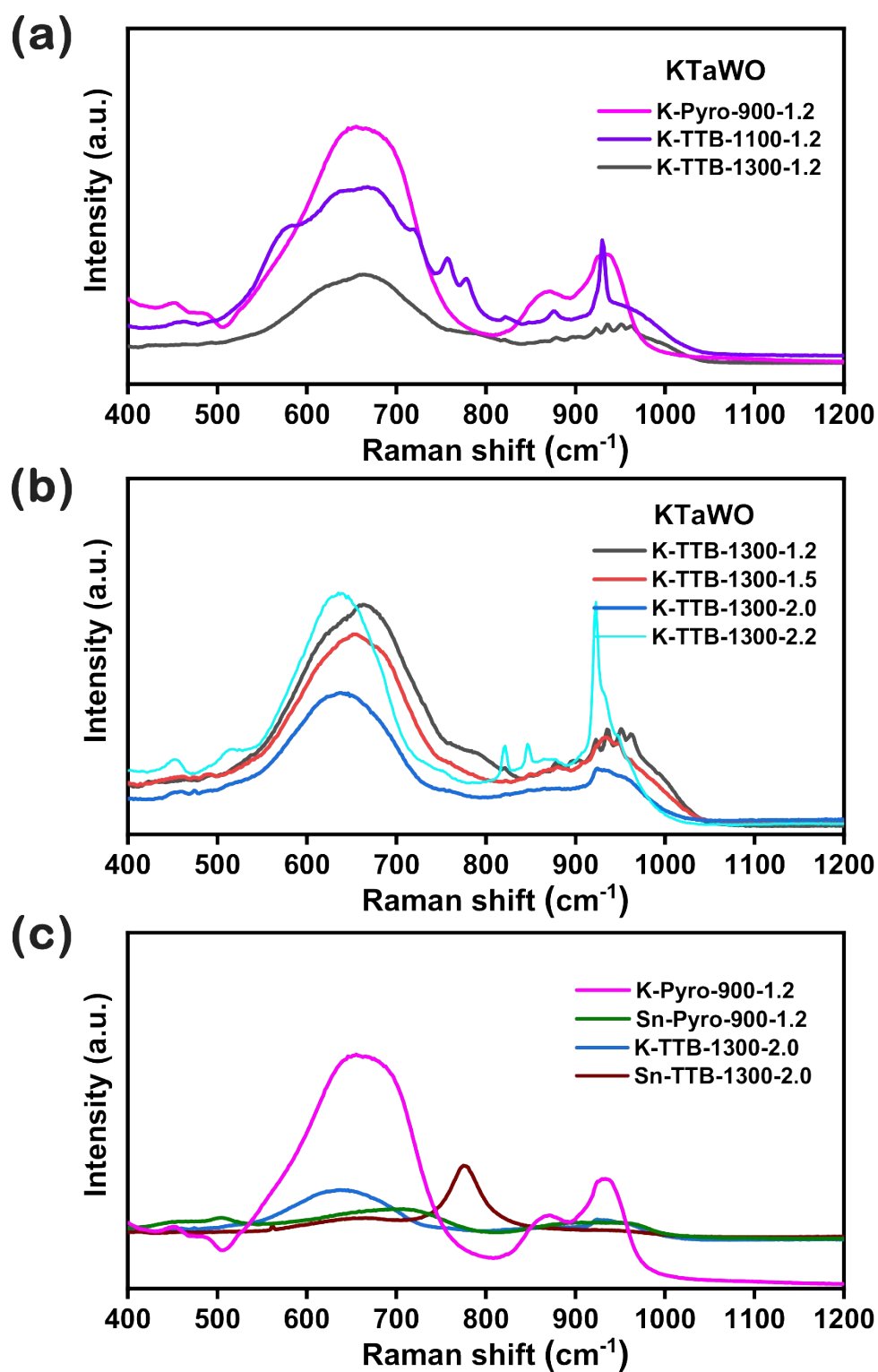


Figure S4. Raman spectra showing the vibrational features of the K-Pyro and K-TTB intermediates prepared at different temperatures and with varied K/Ta ratios and the corresponding Sn(II) ion exchanged products; measurements performed with powder samples stimulated by 532 nm laser.

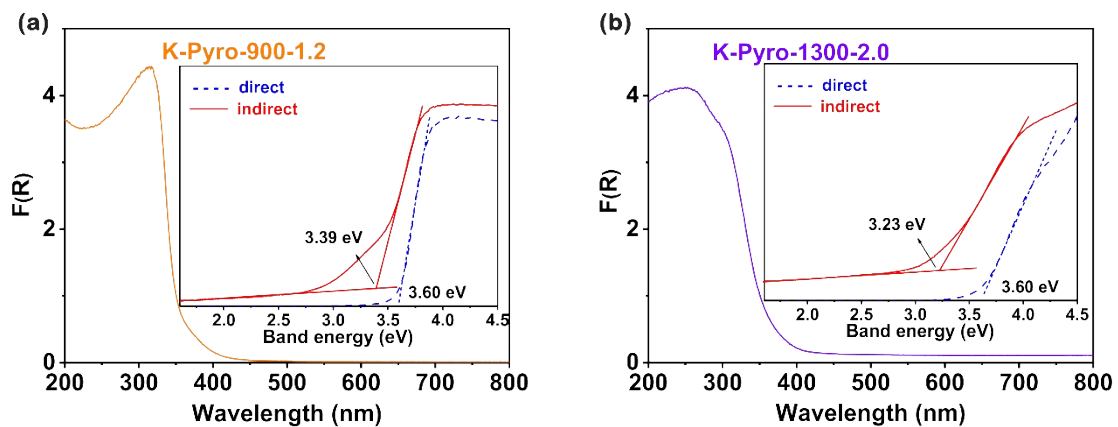


Figure S5. UV-visible diffuse reflectance spectra (DRS) of K-Pyro and K-TTB prepared at different temperatures and with varied K/Ta ratios and the corresponding Tauc plot.

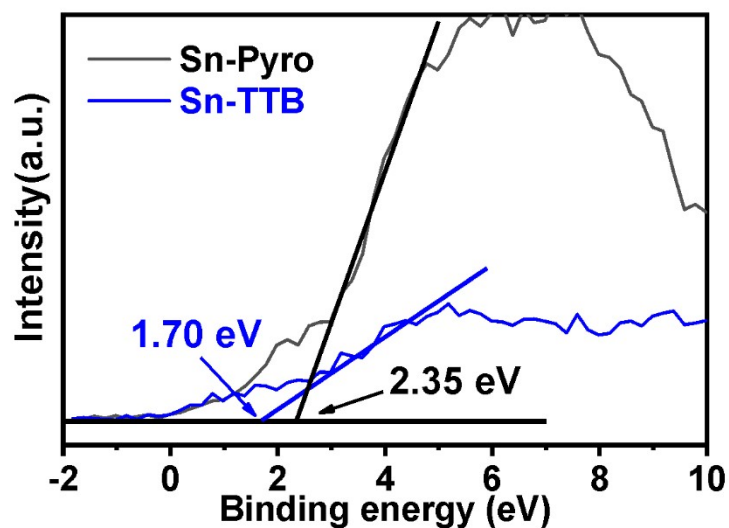


Figure S6. The valence band XPS spectra (VB-XPS) of Sn-Pyro and Sn-TTB.

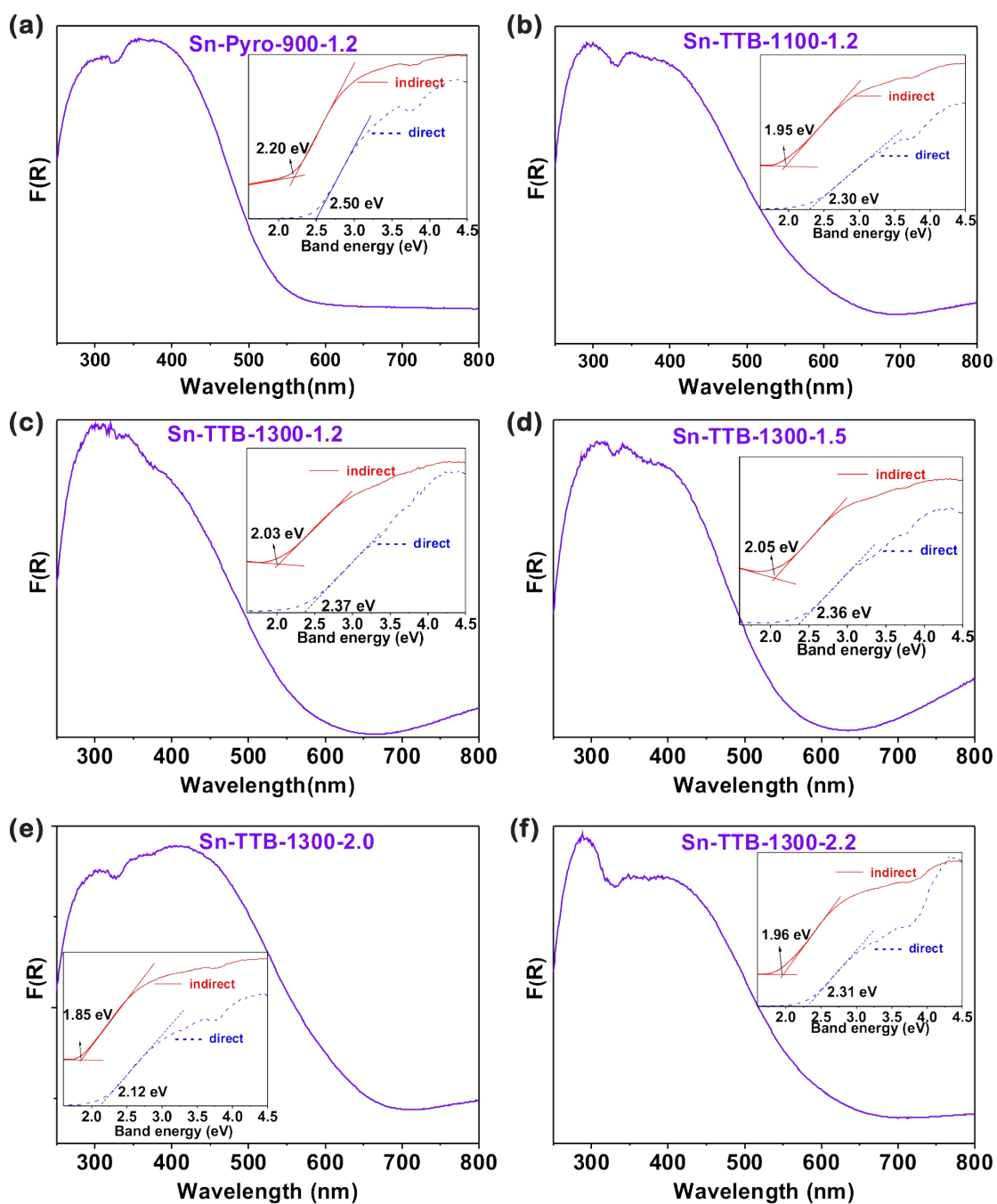


Figure S7. UV-visible diffuse reflectance spectra (DRS) of Sn-Pyro and Sn-TTB prepared at different temperatures and with varied K/Ta ratios and the corresponding Tauc plot.

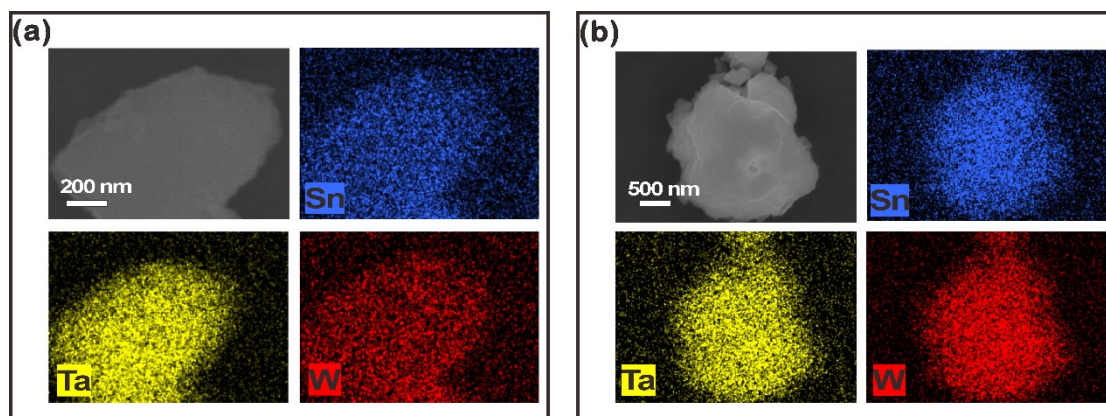


Figure S8. SEM images of EDS face scanning profile of the (a) Sn-TTB and (b) Sn-Pyro.

Table S4 XRF profile of Sn-TTB

Element	Wt %	Atomic percent
Sn	19.0	26.5
Ta	39.9	36.5
W	41.1	37.0
Total content:	100.0	100.0

Table S5 XRF profile of Sn-Pyro

Element	Wt %	Atomic percent
Sn	16.0	22.7
Ta	38.8	36.0
W	45.2	41.3
Total content:	100.0	100.0

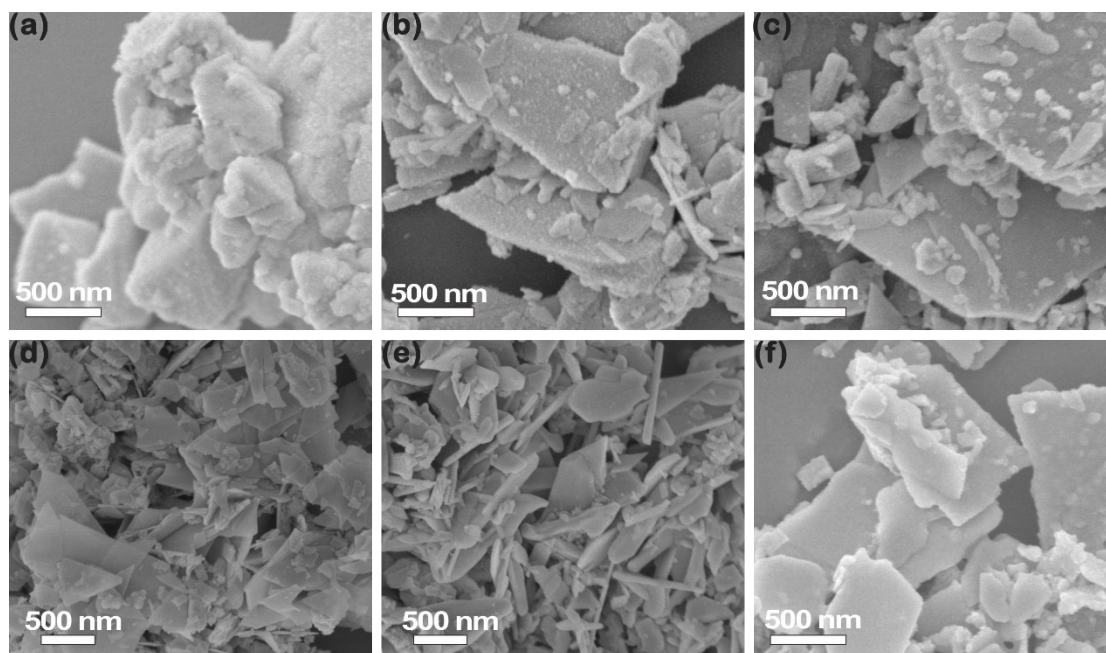


Figure S9. SEM image of Sn- products prepared at different temperatures and with varied K/Ta ratios, (a) Sn-Pyro-900-1.2, (b) Sn-TTB-1100-1.2, (c) Sn-TTB-1300-1.2, (d) Sn-TTB-1300-1.5, (e) Sn-TTB-1300-2.0, (f) Sn-TTB-1300-2.2.

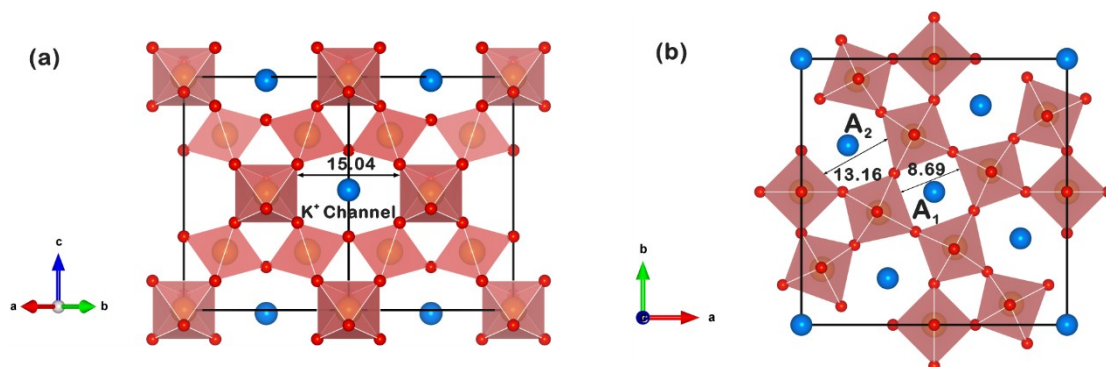


Figure S10. Unit cell structures of K-Pyro (left) and K-TTB (right). Color code: K (blue), Ta/W (orange), and O (red). The cross-sectional area of K channel in K-Pyro structure is about 15.04 (\AA^2), the cross-sectional area of A₁, A₂ site in K-TTB structure are 8.69 and 13.16 (\AA^2), respectively.

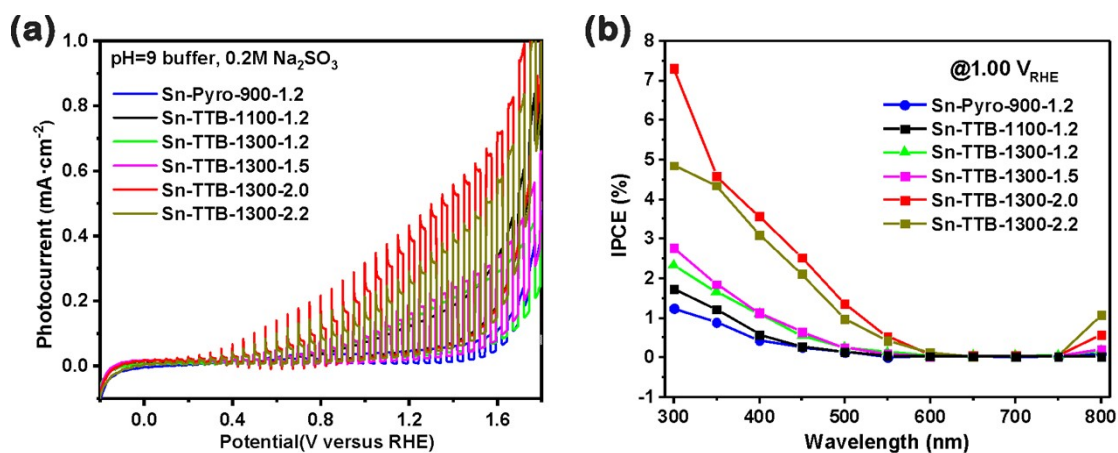


Figure S11. (a) Photocurrent density-potential curves of Sn-Pyro and Sn-TTB products under a chopping AM1.5G illumination, 100 mW/cm², with 0.2 M Na₂SO₃ as the hole scavenger. (b) The incident photon-to-current conversion efficiencies (IPCEs) of Sn-Pyro and Sn-TTB products were measured at 1.00 V_{RHE}.

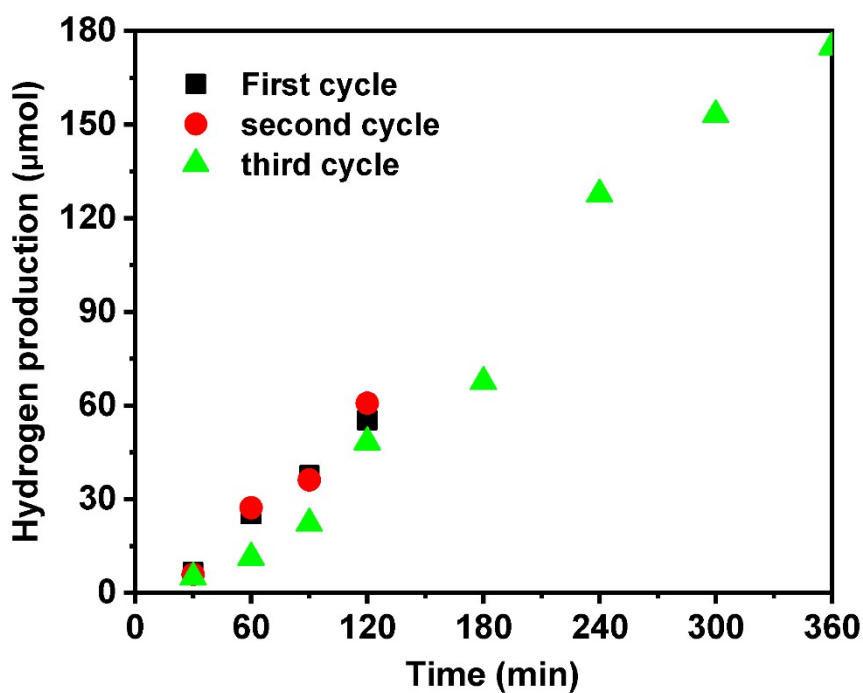


Figure S12. hydrogen evolution detected by gas chromatography in three cycles. All measurements were carried out in a 0.5 M potassium borate electrolyte (pH 9.0) under AM1.5 illumination, 100 mW/cm².

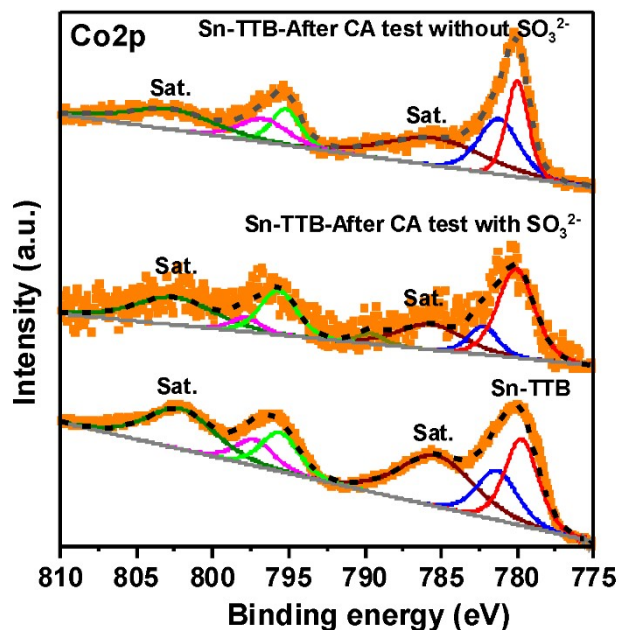


Figure S13. Co2p orbital XPS spectra of Sn-TTB sample (pristine and after CA test). Lorentzian peaks with areas and width constrained were used for fitting core levels of different spins.

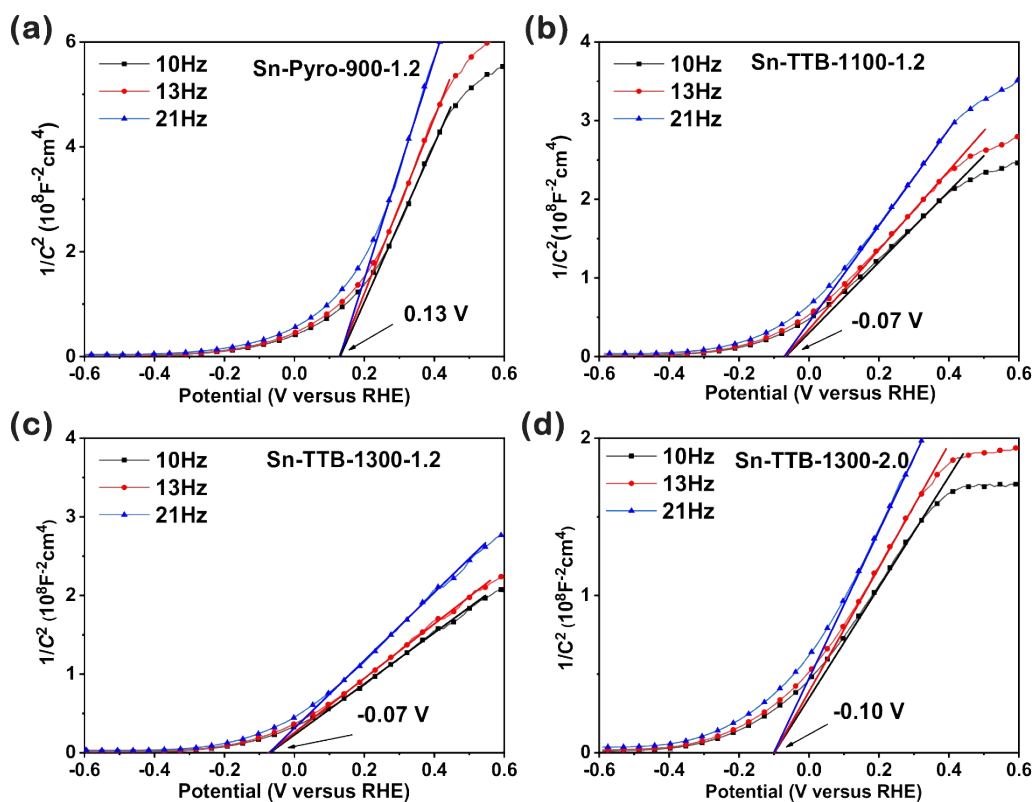


Figure S14. Mott-Schottky plots of (a) Sn-Pyro-900-1.2, (b) Sn-TTB-1100-1.2, (c) Sn-TTB-1300-1.2, (d) Sn-TTB-1300-2.0. The electrochemical tests were performed under aqueous KOH/H₃BO₃ (0.5 M, pH=9.0) buffer in the dark, with a multi-sine data collection mode.

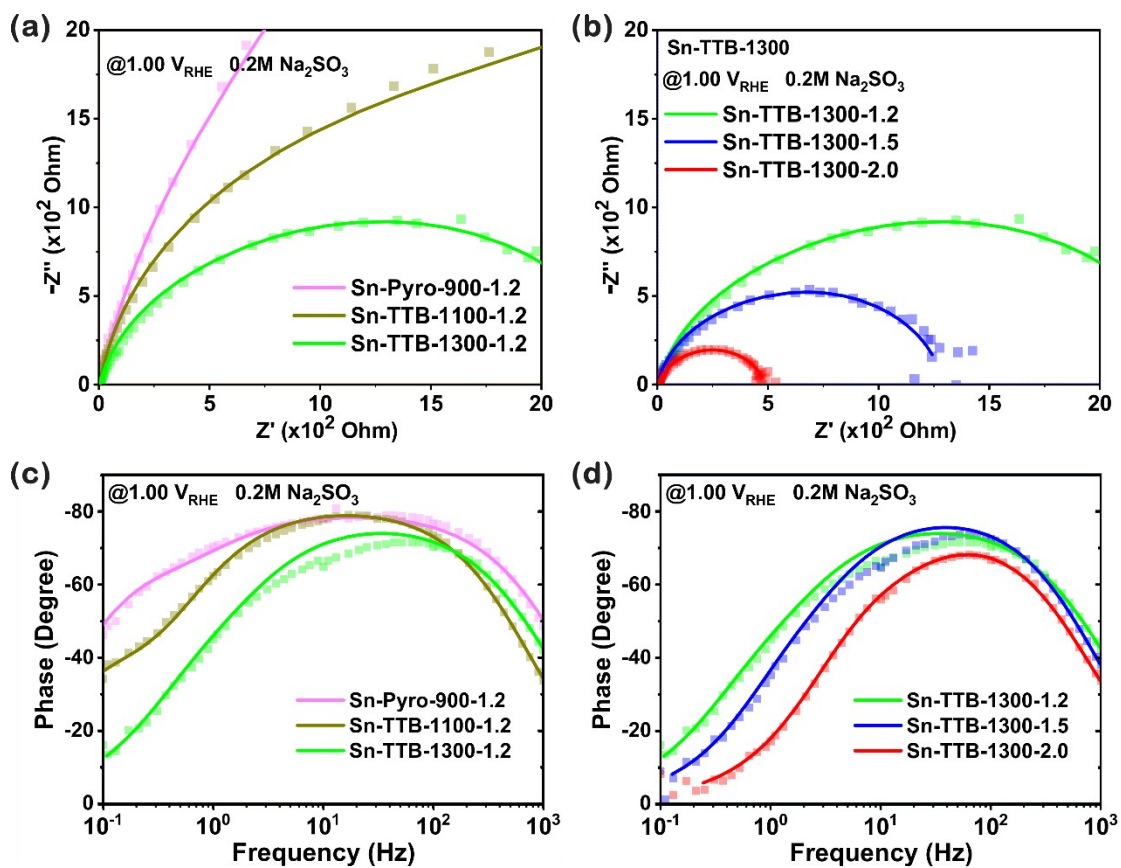


Figure S15. Electrochemical impedance spectra (EIS) measurements. (a,b) The EIS spectra and (c,d) The phase plots of the Sn-Products. The electrochemical tests were performed under aqueous KOH/H₃BO₃ (0.5 M, pH=9.0) buffer with 0.2 M Na₂SO₃ in the presence of LED 455nm light, 39mW/cm². All the samples were decorated with CoOx.

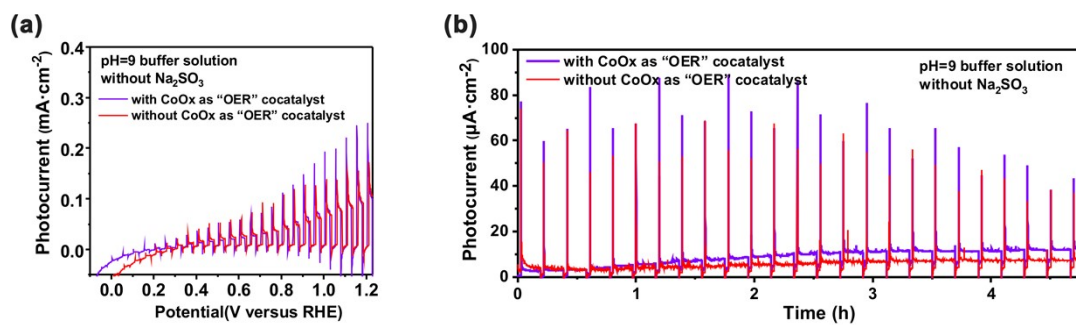


Figure S16. (a) Photocurrent density-potential curves of Sn-TTB products with and without CoOx as “OER” cocatalyst in the absence of the Na_2SO_3 as the hole scavenger with chopping AM1.5G illumination, $100\text{ mW}/\text{cm}^2$. (b) The PEC stability tests of Sn-TTB products with and without CoOx as “OER” cocatalyst in the absence of hole scavenger by chronoamperometric (CA) graphs were measured at $1.00V_{\text{RHE}}$ with chopping AM1.5G illumination, $100\text{ mW}/\text{cm}^2$.